



## Tuning the Liquid-Liquid Transition by Modulating the Hydrogen-Bond Angular Flexibility in a Model for Water

Frank Smallenburg

*Institut für Theoretische Physik II: Weiche Materie, Heinrich-Heine Universität Düsseldorf,  
Universitätstrasse 1, 40225 Düsseldorf, Germany*

Francesco Sciortino

*Department of Physics and CNR-ISC, Sapienza, Università di Roma, Piazzale Aldo Moro 2, I-00185 Roma, Italy*

(Received 9 March 2015; published 1 July 2015)

We propose a simple extension of the well known ST2 model for water [F. H. Stillinger and A. Rahman, *J. Chem. Phys.* 60, 1545 (1974)] that allows for a continuous modification of the hydrogen-bond angular flexibility. We show that the bond flexibility affects the relative thermodynamic stability of the liquid and of the hexagonal (or cubic) ice. On increasing the flexibility, the liquid-liquid critical point, which in the original ST2 model is located in the no-man's land (i.e., the region where ice is the thermodynamically stable phase) progressively moves to a temperature where the liquid is more stable than ice. Our study definitively proves that the liquid-liquid transition in the ST2 model is a genuine phenomenon, of high relevance in all tetrahedral network-forming liquids, including water.

DOI: 10.1103/PhysRevLett.115.015701

PACS numbers: 64.70.Ja, 61.20.Ja

The possibility that a one-component system assumes (beside the gas phase) more than one disordered condensed phase is currently highly debated in liquid state physics. Since the original proposition [1] of a liquid-liquid (LL) transition in supercooled water (based on a molecular dynamics study of the ST2 [2] potential), a large literature body has investigated this topic, suggesting that the microscopic origin of a LL transition must be attributed to the competition between two local structures, differing in energy, entropy, and density [3–14]. Still, when and how the interaction potential between molecules will favor a LL transition that can be accessed in the absence of crystallization is rather unclear. Only recently an effort has been made to provide a picture that simultaneously accounts for the free energy of both the liquid and ordered phases [15–17], as well as of the kinetic barrier separating them. The driving force behind this renewed interest in the physics of LL transitions has been provided by two very controversial studies from the same group [15,18]. These studies state that in previous numerical investigations—including the ST2-based results that originated the LL transition concept—the low-density liquid phase appearing below the LL critical point was in reality an ice phase, i.e., crystallization was mistaken for a LL transition. Several following investigations by different groups have disagreed with this interpretation, providing further support in favor of the presence of two well-defined distinct liquid phases in the ST2 model [16,19–22].

The most recent contribution [16] has confirmed that the free energy basins of the two liquids are well separated from the crystal one and hence, in principle, both liquid phases can be explored in metastable equilibrium

conditions. Of course, this requires that the metastable liquid phases survive without crystallizing for a time longer than the equilibration time. Although this condition was verified in Ref. [16], such times can not be calculated by thermodynamic information only. It is thus worth exploring the possibility of a definitive proof of the existence of a LL critical point in the ST2 model that does not require kinetic information. We present such a proof here by continuously tuning one of the ST2 model parameters. We show that it is possible to modulate the relative stability of the liquid and of the hexagonal (cubic) ice  $I_h$  ( $I_c$ ) such that the melting temperature of  $I_h$  and  $I_c$  drops below the LL critical temperature. Under these conditions, the low-density liquid is thermodynamically more stable than  $I_h$  and  $I_c$ , demonstrating that these two phases are distinct. The results reported in this Letter not only conclude once and for all the debate on the existence of a genuine LL transition in the ST2 model but also provide important clues on the mechanisms controlling crystal stability in tetrahedral lattices.

Our study builds on recent investigations of patchy colloidal particles, interacting via four attractive patches tetrahedrally located on the particle surface [17,23,24]. Searching for the particle properties favoring the self-assembly of the technologically relevant diamond lattice [25], it has been discovered that very flexible bonds destabilize open crystal phases so much that the liquid retains its thermodynamic stability even at very low temperatures [24]. Crystallization is instead favored by highly directional bonds. In addition, at low-temperature  $T$  these systems can exhibit a LL transition between two interpenetrating tetrahedrally coordinated networks [17].

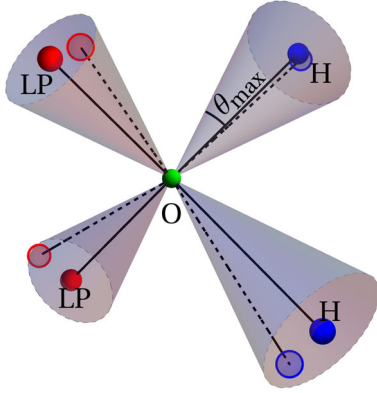


FIG. 1 (color online). Schematic plot of the ST2 water model and of the proposed extension to modulate hydrogen-bond flexibility. Solid lines indicate the position of the H and LP sites in the rigid original ST2 model. The cones have an angular amplitude equal to  $\theta_{\max}$  and define the volume limiting the position of the same sites in the flexible model (dashed lines).

On increasing the bond flexibility the LL transition becomes thermodynamically stable. These results have been confirmed in another colloidal model mimicking DNA constructs with valence 4 [26]. Both colloidal models are characterized by a very large interparticle softness, allowing for full network interpenetration [27]. As a result, the density of the coexisting high-density liquid approximately doubles the density of the low-density liquid phase, a factor significantly larger than what is expected for water. This extreme softness casts some doubt on the applicability of these results to molecular systems and water in particular. We alleviate these doubts here, supporting once more the hypothesis that the liquid-liquid transition is a genuine feature of tetrahedral network forming liquids.

The original ST2 potential envisions a water molecule as a rigid body: the oxygen atom (O) is located at the center, while the two protons (H) are located at a distance of 1 Å from O, forming a fixed  $\angle(\text{H}, \text{O}, \text{H})$  tetrahedral angle. Two sites [mimicking the lone-pairs (LPs)] are located at distance 0.8 Å from O, such that the two O-H and the two O-LP unit vectors form the vertices of a perfect tetrahedron. The H and LP sites carry an electric charge. Long-range electrostatic interactions are included via the reaction field. Complete details of the simulation procedure are as described in Ref. [1]. For this model, the phase diagram has recently been evaluated, demonstrating the stability of  $I_h$  and  $I_c$  at low temperature and pressure [28], consistent with the recent observation of  $I_h$  and  $I_c$  in the simulation of the ST2 model [29]. We modulate the flexibility of the hydrogen bonds by allowing the unit vectors pointing toward the H and LP sites to fluctuate (with no additional energy cost) with respect to the original direction, with a maximum angle  $\theta_{\max}$  (see Fig. 1). By changing  $\theta_{\max}$  it is possible to continuously tune the bond flexibility. When  $\theta_{\max} = 0^\circ$  the modified model coincides with the original ST2 model. Apart from  $\theta_{\max} = 0^\circ$

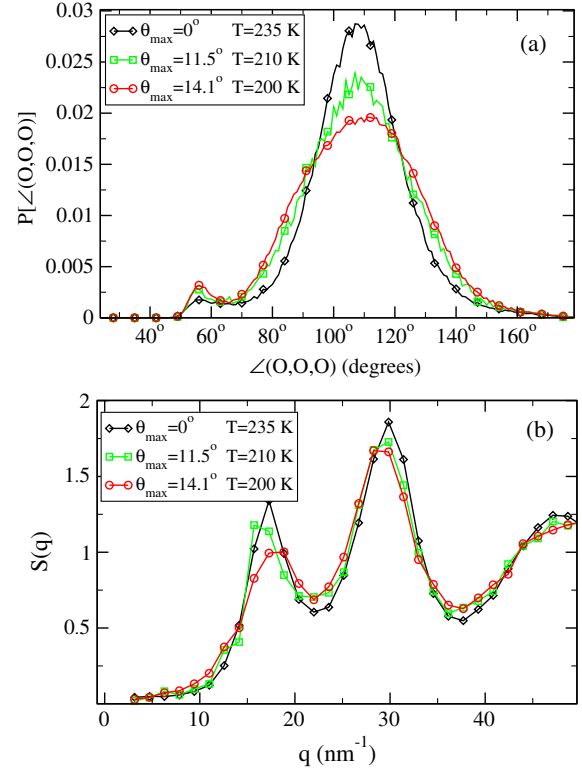


FIG. 2 (color online). (a) Probability distribution of the  $\angle(\text{O}, \text{O}, \text{O})$  angle for bonded triplets at  $\rho = 0.90 \text{ g/cm}^3$  for three different values of the flexibility. Note the increase of the variance of the distribution on increasing flexibility. Two adjacent water molecules are considered bonded if the O-O distance is less than 3.2 Å. (b) Oxygen-oxygen structure factors  $S(q)$  for the same state points, displaying the effect of the flexibility on the prepeak.

( $\cos \theta_{\max} = 1.0$ ), we explore in detail the cases  $\theta_{\max} = 8.11^\circ$  ( $\cos \theta_{\max} = 0.99$ ) and  $\theta_{\max} = 11.5^\circ$  ( $\cos \theta_{\max} = 0.98$ ), and the case  $\theta_{\max} = 14^\circ$  ( $\cos \theta_{\max} = 0.97$ ). We note that, in principle, an energy cost to bending could be included in the model. However, the main effect of this would be to make the effective bond flexibility temperature dependent, and we have thus omitted this here.

To provide evidence that on increasing  $\theta_{\max}$ , the tetrahedral network becomes more and more flexible we evaluate the  $\angle(\text{O}, \text{O}, \text{O})$  angle distribution  $P[\angle(\text{O}, \text{O}, \text{O})]$  between bonded triplets and the structure factor  $S(q)$ , at the lowest  $T$  we have been able to equilibrate and at the optimal network density. Previous studies have shown that the width of  $P[\angle(\text{O}, \text{O}, \text{O})]$  as well as the amplitude of the prepeak in  $S(q)$  correlate with bond flexibility [30]. Figure 2 shows that the angular distribution is centered around the tetrahedral angle but widens on increasing  $\theta_{\max}$ , indicating the larger number of geometrical arrangements available for the formation of the network. Simultaneously, the larger disorder in the network structure decreases the intensity of the  $S(q)$  prepeak, in full agreement with results based on tetrahedral patchy colloids [30].

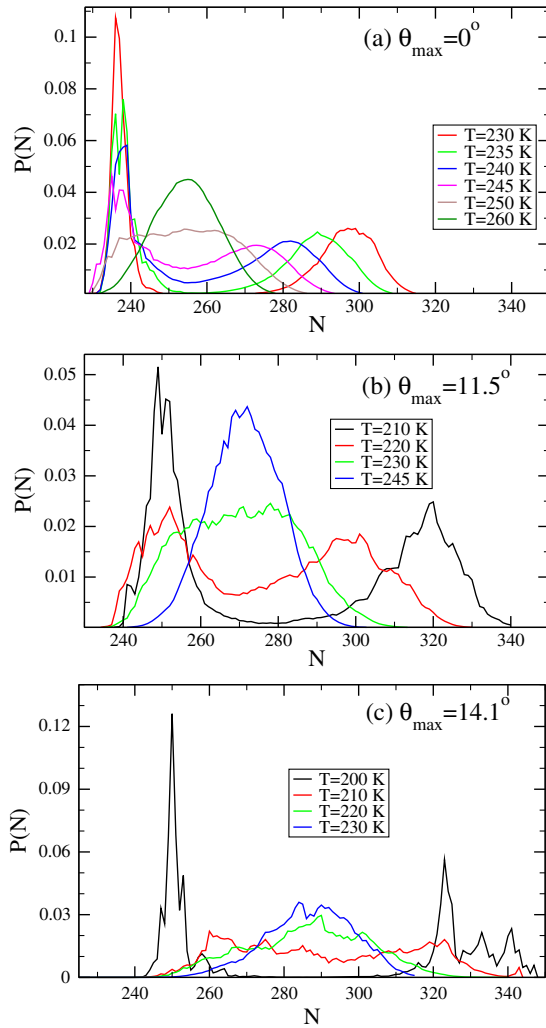


FIG. 3 (color online). Distribution  $P(N)$  in the number  $N$  of particles populating a volume of  $8 \text{ nm}^3$  at fixed temperature and chemical potential  $\mu$ , for three different bond flexibilities  $\theta_{\max} = 0^\circ$  (a),  $\theta_{\max} = 11.5^\circ$  (b) and  $\theta_{\max} = 14^\circ$  (c). This last quantity controls the average density and it is selected to provide equal area below the low-density and high-density liquid phases.  $P(N)$  evolves from a single-peak to a double peak shape on crossing  $T_c^{\text{LL}}$ . The data for (a) are redrawn from Ref. [19].

To estimate the location of the LL critical point we perform grand-canonical Monte Carlo simulations for different  $T$  to estimate the probability  $P(N)$  of finding  $N$  particles in the simulated volume  $V$  ( $8 \text{ nm}^3$ ). By implementing the successive umbrella sampling technique [31], we have distributed the evaluation of  $P(N)$  over multiple processors, each of them evaluating the ratio  $P(N+1)/P(N)$ , for  $220 < N < 350$ . More than 1000 processors running full time have been dedicated for six months to these calculations. Close to a second-order critical point,  $P(N)$  develops a double peak structure that becomes more and more pronounced on cooling, signalling the coexistence of phases with different density. During all runs, we have constantly checked that the number of crystalline

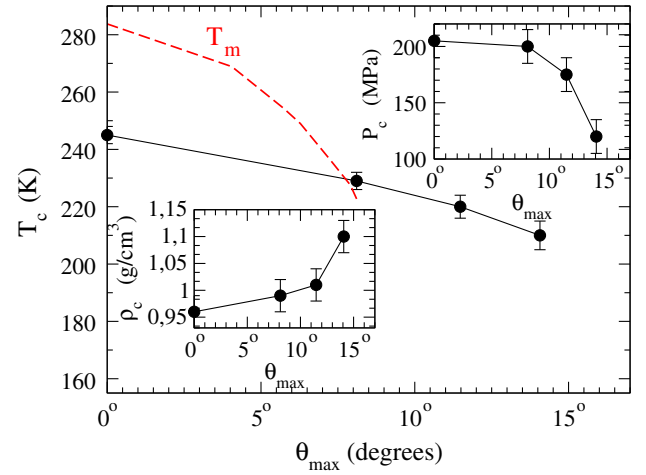


FIG. 4 (color online). Dependence of the liquid-liquid critical point temperature  $T_c^{\text{LL}}$  on bond flexibility calculated from the free energy estimate based on successive umbrella sampling simulations. These grand-canonical simulations are performed for a volume of  $8 \text{ nm}^3$ . The dashed red line indicates  $T_m$ , the melting  $T$  for the liquid to  $I_h$  and  $I_c$  transformation at the critical pressure. The two insets show, respectively, the critical pressure  $P_c$  and the critical density  $\rho_c$  as a function of  $\theta_{\max}$ .

particles (evaluated with the standard algorithms for detecting ice local structures [23,32]) never exceeded 10 or showed any trend toward growing. The results of these calculations for different  $\theta_{\max}$  and  $T$  are reported in Fig. 3, spanning the  $T$  interval over which  $P(N)$  crosses from a single- to a double-peaked function with a peak-to-valley ratio of around 0.5 [the characteristic value assumed by  $P(N)$  at the critical temperature [33]] down to  $T$  where the two peaks are well resolved, signalling the onset of a clear free energy barrier between the low-density and high-density liquids. The estimated location of the critical temperature  $T_c^{\text{LL}}$  for the investigated box side ( $L = 2 \text{ nm}$ ) as a function of  $\theta_{\max}$  is shown in Fig. 4. Consistent with what was previously found for the patchy and DNA colloidal models, increasing bond flexibility (i.e., increasing  $\theta_{\max}$ ) results in lowering  $T_c^{\text{LL}}$ . Additionally, upon increasing the flexibility, the critical pressure decreases and the critical density increases, consistent with the coupling between bond flexibility and local density. Indeed, for tetrahedral patchy particles it has been shown that the density at zero pressure of the fully bonded network decreases with increasing bond directionality. Similarly, increasing flexibility results in a network that is much more easily compressible [30]. Our results suggest that the coupling between local density, compressibility, and flexibility also affects the critical parameters.

To properly frame the LL transition in terms of the thermodynamic stability compared to  $I_h$  and  $I_c$  we evaluate the free energy of the liquid and of the two ices. To evaluate the liquid free energy, we perform a thermodynamic integration from the ideal gas [28]. To evaluate the crystal

free energy we integrate from an Einstein crystal in the molecular framework [34], extending the method to account for the flexible arms. For this, we use as a reference system a thermalized  $I_h$  or  $I_c$  configuration with at least 20 000 particles to average over proton disorder. For each molecule in the reference system we define the reference oxygen position  $\mathbf{r}_0$ , the reference orientation of the dipole and H-H unit vectors, and the reference orientation of the O-H and O-LP unit vectors, all in the ideal tetrahedral geometry. For each particle, the reference Hamiltonian consists of three parts:

$$H_{\text{trans}} = \lambda_r (|\mathbf{r} - \mathbf{r}_0|)^2 / \sigma^2, \quad (1)$$

$$H_{\text{rot}} = \lambda_r \left[ \sin^2 \phi_a + \left( \frac{\phi_b}{\pi} \right)^2 \right], \quad (2)$$

$$H_{\text{arms}} = \lambda_a \sum_{i=1}^4 [1 - \cos \theta_i], \quad (3)$$

where  $|\mathbf{r} - \mathbf{r}_0|$  is the distance between the position of the oxygen atom in the reference and in the instantaneous configuration,  $\sigma = 1$  nm is a convenient length scale,  $\phi_a$  and  $\phi_b$  are, respectively, the angle between the reference and the instantaneous position of the ideal dipole and H-H unit vectors, and  $\theta_i$  is the angle between the instantaneous position of the  $i$  patch unit vector and the ideal position of that unit vector. In other words, this is the angle we limit in our model when specifying  $\theta_{\text{max}}$ .

Monte Carlo moves, preserving the center of mass position [35], are performed by randomly translating a molecule, rotating a single patch (which changes only  $H_{\text{arms}}$ ), or rigidly rotating the water molecule (which changes only  $H_{\text{rot}}$ ).

The reference free energy (per particle) of the fully constrained system (limit of high  $\lambda$ ) is (with  $\beta = 1/k_B T$  and  $k_B$  the Boltzmann constant)

$$\beta f_{\text{ref}} = \beta f_{\text{trans}} + \beta f_{\text{rot}} + 4\beta f_{\text{arm}} \quad (4)$$

with

$$\beta f_{\text{trans}} = -\frac{1}{N} \log \left[ \left( \frac{\pi}{\beta \lambda_r} \right)^{3(N-1)/2} N^{3/2} \frac{V}{\sigma^3 N} \right], \quad (5)$$

$$\beta f_{\text{rot}} = -\log [\sqrt{\pi}/4] + \frac{3}{2} \log(\beta \lambda_r), \quad (6)$$

$$\beta f_{\text{arm}} = -\log \left[ \frac{(1 - \exp[-\beta \lambda_a (1 - \cos \theta_{\text{max}})])}{(1 - \cos \theta_{\text{max}}) \beta \lambda_a} \right] \quad (7)$$

$$\approx \log((1 - \cos \theta_{\text{max}}) \beta \lambda_a). \quad (8)$$

The model free energy  $f$  is then calculated following the methodology described in Ref. [34]. As for the original ST2

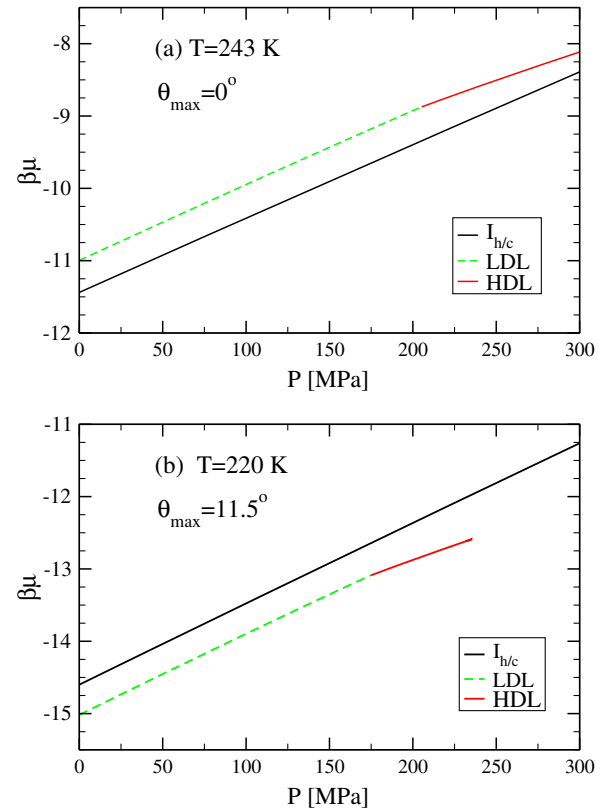


FIG. 5 (color online). Pressure  $P$  dependence of the reduced chemical potential  $\beta\mu$  for  $I_h$  and  $I_c$  and for the low- and high-density liquid phases at  $T_c^{\text{LL}}$  for (a)  $\theta_{\text{max}} = 0^\circ$  and (b)  $\theta_{\text{max}} = 11.5^\circ$ . Note that while for  $\theta_{\text{max}} = 0^\circ$  (e.g., for the original ST2 model)  $\beta\mu$  of the liquid phases is higher than the one of  $I_h$  and  $I_c$ ; the opposite is found already for  $\theta_{\text{max}} = 11.5^\circ$ . Under these conditions, the liquid is thermodynamically more stable than  $I_h$  and  $I_c$ .

model, at all temperatures and for all values of  $\theta_{\text{max}}$ , we find that  $I_h$  and  $I_c$  have the same free energies, within our numerical precision (with an uncertainty in  $\beta f$  of  $\pm 0.01$ ). From the free energy and the equation of state we evaluate the chemical potential  $\beta\mu = \beta f + \beta P/\rho$ , where  $P$  is the pressure and  $\rho$  is the number density. The main results of the Letter are reported in Fig. 5, showing the  $P$  dependence of the liquid and  $I_h$  and  $I_c$  chemical potential at the LL critical temperature  $T_c^{\text{LL}}$ . In the case of the original ST2 model ( $\theta_{\text{max}} = 0^\circ$ ),  $\beta\mu$  of  $I_h$  and  $I_c$  is always lower than the liquid one, consistent with the location of  $T_c^{\text{LL}}$  in the no-man's land. On increasing  $\theta_{\text{max}}$ , the relative stability of  $I_h$  and  $I_c$  compared to the liquid changes. At  $\theta_{\text{max}} \approx 8^\circ$ , the liquid chemical potential is slightly lower than  $I_h$  and  $I_c$ , while for  $\theta_{\text{max}} = 11.5^\circ$  at  $T_c^{\text{LL}}$  the liquid phase has gained a significant stability compared to the open crystal lattice. Since the crystal free energy is higher than the liquid one (already for  $\theta_{\text{max}} \approx 8^\circ$ ) there is no possibility that the low-density liquid phase in the flexible ST2 model will ever convert into the  $I_h$  and  $I_c$  structure. The low-density liquid phase is, without any ambiguity, a phase by itself,

definitively disproving the arguments in Refs. [15,18]. In an expanded representation of the phase diagram, in which we include  $T$ ,  $P$ , and  $\theta_{\max}$ , the lines of LL critical points move with continuity from a condition of metastability with respect to  $I_h$  and  $I_c$  to a condition of stability, around  $\theta_{\max} = 8^\circ$ . This continuity allows us to conclude that the LL critical point observed in the original ST2 model must also be genuine. We stress that our study does not aim at providing a (better or worse) model for water but to show—with an extremely simple modification to the ST2 model—that the liquid-liquid transition can be made thermodynamically stable. For the case of water, the estimated LL critical point is definitively located in the region in which ice nucleation in the bulk is dominant. There, only ingenious experiments in the negative pressure region of the phase diagram [36,37] or in the low- $T$  glass phases [6] can provide important clues. Still, our proof reinforces the idea that the LL transition is a genuine phenomenon in all tetravalent systems for which a suitable softness allows for network interpenetration and a suitable bond flexibility allows for enhanced stability of the liquid phase(s) compared to open crystal structures.

We thank P. Debenedetti and L. Filion for discussion and comments.

- 
- [1] P. H. Poole, F. Sciortino, U. Essmann, and H. E. Stanley, *Nature (London)* **360**, 324 (1992).
- [2] F. H. Stillinger and A. Rahman, *J. Chem. Phys.* **60**, 1545 (1974).
- [3] P. Debenedetti and H. Stanley, *Phys. Today* **56**, No. 6, 40 (2003).
- [4] P. G. Debenedetti, *J. Phys. Condens. Matter* **15**, R1669 (2003).
- [5] O. Mishima and H. E. Stanley, *Nature (London)* **396**, 329 (1998).
- [6] K. Amann-Winkel, C. Gainaru, P. H. Handle, M. Seidl, H. Nelson, R. Böhmer, and T. Loerting, *Proc. Natl. Acad. Sci. U.S.A.* **110**, 17720 (2013).
- [7] D. A. Fuentevilla and M. A. Anisimov, *Phys. Rev. Lett.* **97**, 195702 (2006).
- [8] M. J. Cuthbertson and P. H. Poole, *Phys. Rev. Lett.* **106**, 115706 (2011).
- [9] A. Taschin, P. Bartolini, R. Eramo, R. Righini, and R. Torre, *Nat. Commun.* **4**, 2401 (2013).
- [10] G. Franzese, G. Malescio, A. Skibinsky, S. V. Buldyrev, and H. Stanley, *Nature (London)* **409**, 692 (2001).
- [11] H. Tanaka, *Phys. Rev. E* **62**, 6968 (2000).
- [12] P. Gallo and F. Sciortino, *Phys. Rev. Lett.* **109**, 177801 (2012).
- [13] J. Russo and H. Tanaka, *Nat. Commun.* **5**, 3356 (2014).
- [14] V. Holtén, J. C. Palmer, P. H. Poole, P. G. Debenedetti, and M. A. Anisimov, *J. Chem. Phys.* **140**, 104502 (2014).
- [15] D. T. Limmer and D. Chandler, *J. Chem. Phys.* **135**, 134503 (2011).
- [16] J. C. Palmer, F. Martelli, Y. Liu, R. Car, A. Z. Panagiotopoulos, and P. G. Debenedetti, *Nature (London)* **510**, 385 (2014).
- [17] F. Smallenburg, L. Filion, and F. Sciortino, *Nat. Phys.* **10**, 653 (2014).
- [18] D. T. Limmer and D. Chandler, *J. Chem. Phys.* **138**, 214504 (2013).
- [19] F. Sciortino, I. Saika-Voivod, and P. H. Poole, *Phys. Chem. Chem. Phys.* **13**, 19759 (2011).
- [20] P. H. Poole, R. K. Bowles, I. Saika-Voivod, and F. Sciortino, *J. Chem. Phys.* **138**, 034505 (2013).
- [21] T. Kesselring, G. Franzese, S. Buldyrev, H. Herrmann, and H. E. Stanley, *Sci. Rep.* **2**, 474 (2012).
- [22] Y. Liu, J. C. Palmer, A. Z. Panagiotopoulos, and P. G. Debenedetti, *J. Chem. Phys.* **137**, 214505 (2012).
- [23] F. Romano, E. Sanz, and F. Sciortino, *J. Chem. Phys.* **134**, 174502 (2011).
- [24] F. Smallenburg and F. Sciortino, *Nat. Phys.* **9**, 554 (2013).
- [25] M. Maldovan and E. L. Thomas, *Nat. Mater.* **3**, 593 (2004).
- [26] F. W. Starr and F. Sciortino, *Soft Matter* **10**, 9413 (2014).
- [27] C. W. Hsu, J. Largo, F. Sciortino, and F. W. Starr, *Proc. Natl. Acad. Sci. U.S.A.* **105**, 13711 (2008).
- [28] F. Smallenburg, P. H. Poole, and F. Sciortino, *Mol. Phys.* (2015).
- [29] T. Yagasaki, M. Matsumoto, and H. Tanaka, *Phys. Rev. E* **89**, 020301 (2014).
- [30] I. Saika-Voivod, F. Smallenburg, and F. Sciortino, *J. Chem. Phys.* **139**, 234901 (2013).
- [31] P. Virnau and M. Müller, *J. Chem. Phys.* **120**, 10925 (2004).
- [32] P. Bolhuis and D. Frenkel, *J. Chem. Phys.* **106**, 666 (1997).
- [33] N. B. Wilding, *Phys. Rev. E* **52**, 602 (1995).
- [34] C. Vega, E. Sanz, J. Abascal, and E. Noya, *J. Phys. Condens. Matter* **20**, 153101 (2008).
- [35] D. Frenkel and B. Smit, *Understanding Molecular Simulation: From Algorithms to Applications*, Vol. 1 (Academic Press, New York, 2001).
- [36] M. E. M. Azouzi, C. Ramboz, J.-F. Lenain, and F. Caupin, *Nat. Phys.* **9**, 38 (2013).
- [37] G. Pallares, M. E. M. Azouzi, M. A. González, J. L. Aragonés, J. L. Abascal, C. Valeriani, and F. Caupin, *Proc. Natl. Acad. Sci. U.S.A.* **111**, 7936 (2014).